Available online at www.sciencedirect.com
SCIENCE DIRECT®
Thin Solid Films 430 (2003) 292–295
thin solid films
www.elsevier.com/locate/tsf

Hot-wire chemical vapor deposition of carbon nanotubes

A.C. Dillon*, A.H. Mahan, J.L. Alleman, M.J. Heben, P.A. Parilla, K.M. Jones

National Renewable Energy Laboratory, 1617 Cole Blvd, Golden, CO 80401, USA

Abstract

Hot-wire chemical vapor deposition (HWCVD) has been employed for the continuous gas-phase generation of both carbon multi-wall and single-wall nanotube (MWNT and SWNT) materials. Graphitic MWNTs were produced at a very high density at a synthesis temperature of ~600 °C. SWNTs were deposited at a much lower density on a glass substrate held at 450 °C. SWNTs are typically observed in large bundles that are stabilized by tube–tube van der Waals' interactions. However, transmission electron microscopy analyses revealed only the presence of isolated SWNTs in these HWCVD-generated materials.
© 2003 Elsevier Science B.V. All rights reserved.

Keywords: Hot-wire chemical vapor deposition (HWCVD); Carbon multi-wall nanotubes (MWNTs); Carbon single-wall nanotubes (SWNTs); Ferrocene

1. Introduction

Both carbon multi-wall (MWNTs) and single-wall nanotubes (SWNTs) hold great promise for a wide variety of applications. For example, carbon nanotubes may be employed in the fabrication of strong composite materials, nano-scale electronic devices and adsorbents for gas separation or storage applications. The development of a low-cost scalable production method has therefore been a major research priority. Densely packed MWNTs have been grown on supported metal catalyst particles or films via hot-wire chemical vapor deposition (HWCVD) [1,2] and plasma-enhanced HWCVD methods [3,4]. A recent HWCVD report employed the in situ evaporation of an Fe–Cr filament to supply a metal catalyst. Gas-phase production of MWNTs was demonstrated. However, a relatively high density of structural defects was indicated by Raman spectroscopy [5]. Finally, HWCVD has been employed to grow bundles of SWNTs between metallic contacts, forming a nano-scale conducting network [6].

This paper demonstrates HWCVD continuous gas-phase production of both MWNT and SWNT materials. Using methane as a carbon source and ferrocene to supply a metal catalyst, a hot filament operating at ~2000 °C is sufficient to decompose the gas-phase precursors without an additional plasma. Graphitic MWNTs were observed at an exceptionally high yield in a quartz tube reactor held at ~600 °C. SWNTs were deposited at much lower yield on a glass substrate at 450 °C. However, although SWNTs are typically observed in large bundles stabilized by tube–tube van der Waals' interactions, transmission electron microscopy (TEM) analyses revealed only the presence of isolated SWNTs in these HWCVD-generated materials [7].

2. Experimental details

A 0.5-mm tungsten filament was operated between 20 and 25 A, at ~20 V and ~2000 °C in a static gas atmosphere of 1:5 CH_4/H_2 at 150 Torr. Carbon nanotube growth is catalyzed by transition metal particles. Once nucleation occurs on the metal particle surface, growth in the tube length may rapidly occur as more carbon atoms are added. Often, the nanotube diameter corresponds to the size of the metal catalyst particle. In these HWCVD experiments, ferrocene was employed to supply a gas-phase iron catalyst by maintaining the powder source near the sublimation temperature of 140 °C throughout nanotube syntheses. The MWNT-containing material was grown within a 2-inch-diameter quartz tube heated to ~600 °C with a clamshell furnace [8]. The SWNT-containing material was deposited on a glass

*Corresponding author. Tel.: +1-303-384-6607; fax: +1-303-384-6655.
E-mail address: adillon@nrel.gov (A.C. Dillon).

0040-6090/03/$ - see front matter © 2003 Elsevier Science B.V. All rights reserved.
doi:10.1016/S0040-6090(03)00084-1

substrate, heated to 450 °C and located approximately 1 inch from the filament inside a separate, previously described chamber [9].

Samples were prepared for TEM by suspending ~0.2 mg of the material in 10 ml of acetone. The solutions were sonicated for 5 min and ~6 drops were placed on Ted Pella ultra-thin carbon type-A 400-mesh grids. For the SWNT material, small pieces of dry sample extracted from the glass substrate were also mounted directly on grids in order to confirm that the sample preparation process did not effect the SWNT bundling. Raman spectroscopy was performed in a backscattering configuration with a resolution of 2–4 cm^{-1} using ~7 mW of the 488-nm line of an Ar ion laser.

3. Results and discussion

Employing the quartz tube reactor and an external synthesis temperature of ~600 °C, a carbon film containing a very high density of multi-wall carbon nanotubes was produced. Fig. 1a displays a TEM image of a mat of MWNTs contained in the deposited film. Small iron catalyst particles with diameters of ~10–20 nm are also clearly observed in the TEM image, but very few carbon impurities are detected in this or other images of the MWNT material. Fig. 1b displays a higher-resolution TEM image of the HWCVD-generated multi-wall tubes. This image indicates that the nanotubes have hollow inner cavities and walls that are several nm in thickness. Closer inspection confirms that the nanotubes are highly graphitic, containing ~3–20 concentric shells with inner and outer tube diameters of ~4–15 and ~6–20 nm, respectively. The spacing between shells measures ~3.4 Å, corresponding to the distance between the planes in (002) graphite. Furthermore, Raman spectroscopy indicates a relatively low concentration of defects in the graphitic walls [8]. The density of the multi-wall nanotubes produced in this iron-catalyzed gas-phase process also appears similar to the values reported for carbon nanotubes deposited on Ni-coated substrates [1–4].

Following extensive TEM analysis of the HWCVD-generated SWNT-containing materials, it was only possible to find isolated nanotubes. Fig. 2a displays a TEM image of an isolated SWNT found in a HWCVD-deposited film. Measurements of ~20 images of different isolated tubes showed the SWNT diameter range to be 1.1–1.5 nm. In general, SWNTs form bundles of nanotubes during synthesis, stabilized by tube–tube van der Waals' interactions. For comparison, Fig. 2b displays a TEM image of a large bundle of purified [10] SWNTs formed by the laser vaporization of a Co/Ni-doped graphite target [11]. An image of the purified material is shown so that the tube walls are more clearly resolved. The purification process does not significantly alter the bundle size of the as-produced nanotubes. The unique

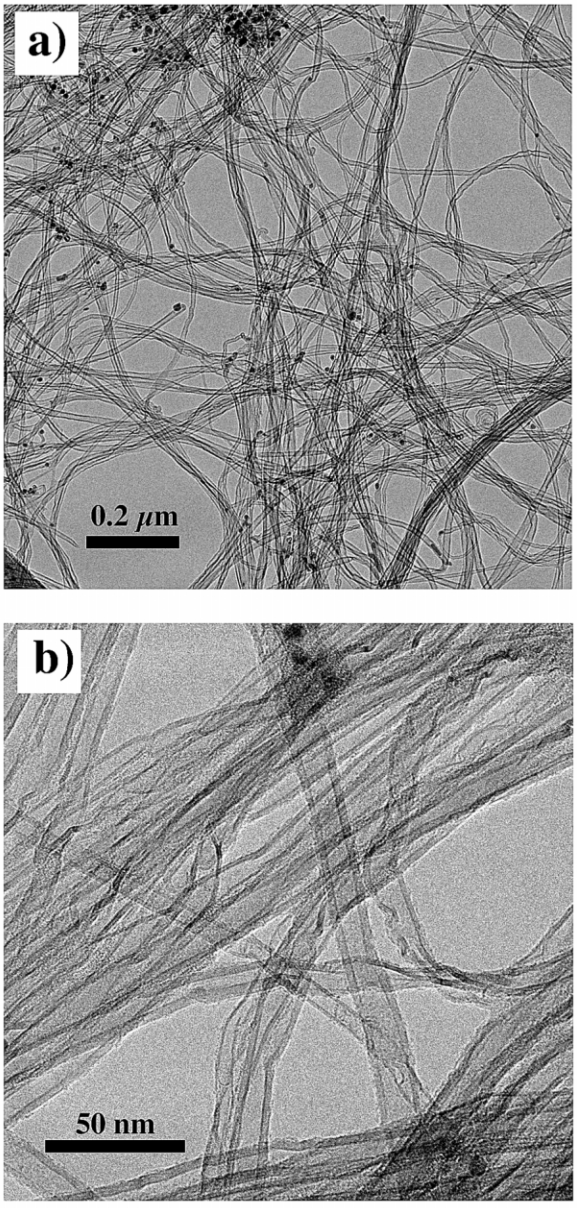

Fig. 1. TEM images of (a) a mat of HWCVD-generated multi-wall carbon nanotubes; and (b) the same nanotubes at a higher magnification.

formation of isolated SWNTs observed with this HWCVD process may be attributed to either a very short SWNT formation period, as the SWNTs were deposited approximately 1 inch from the filament, or to the fact that HWCVD species are generally negatively charged [12]. Details of the possible formation mechanisms that could result in isolated SWNTs have been provided elsewhere [7].

Fig. 3a displays the Raman spectrum of the characteristic SWNT tangential bands at 1593 and 1571 cm^{-1} for the HWCVD film. A broad disorder band at 1350 cm^{-1} is apparent, indicating the presence of amorphous carbon and nanocrystalline graphite impuri-

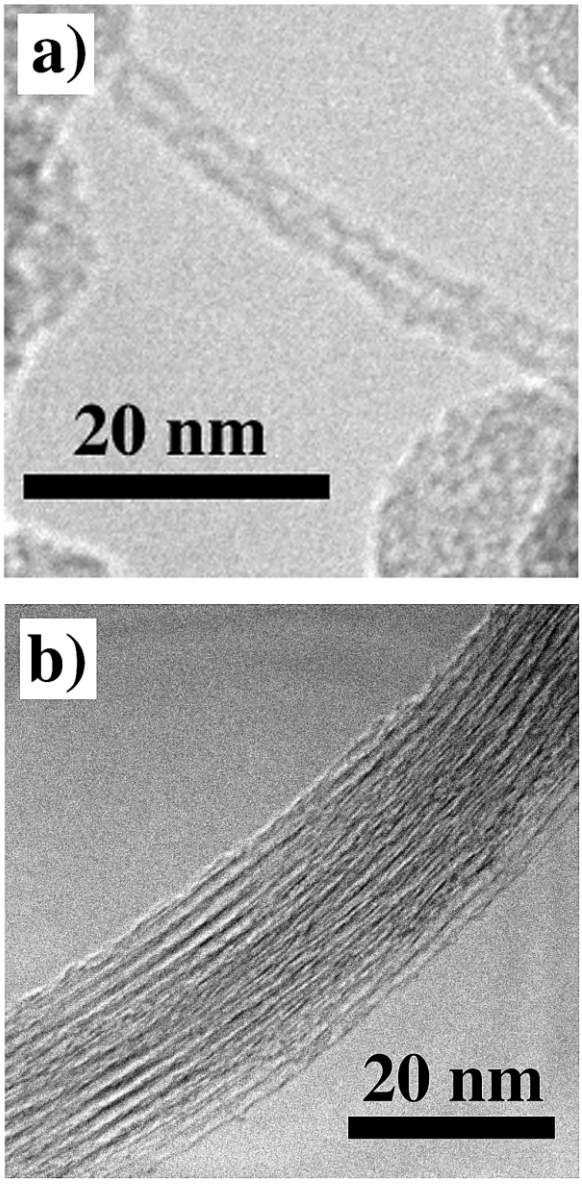

Fig. 2. TEM images of (a) an isolated single-wall carbon nanotube produced via HWCVD and (b) a bundle of purified laser-generated SWNTs.

ties [10]. A reduction in carbon impurities should occur with further optimization of the process, such as employing a dual catalyst mixture. Fig. 3b displays the Raman spectrum of the material between 150 and 350 cm^{-1}. The features in this region are attributed to the SWNT radial breathing modes, and their frequencies are diameter-dependent [13]. The frequencies of the radial breathing modes for all SWNTs have been shown to fall on the line $\omega(d) = 223.75/d$, where ω is in units of cm^{-1} and d corresponds to the tube diameter in nm [14]. The spectral features in Fig. 3b are then consistent with a diameter distribution of $\sim$0.9–1.4 nm [14], and the dominant feature at 183 cm^{-1} corresponds to nanotubes that are 1.2 nm in diameter. It is, however, possible that nanotubes of a different diameter would be predominant and/or a different diameter range would be observed if a different wavelength were employed in the Raman excitation.

4. Conclusions

In summary, a simple, scalable, continuous HWCVD process for the gas-phase growth of MWNT and SWNT materials has been demonstrated. Well-graphitized MWNTs were produced at very high yield. The nanotubes are comprised of $\sim$3–20 concentric shells with inner and outer tube diameters of $\sim$4–15 and $\sim$6–20 nm, respectively. The SWNTs were produced at much lower density and were found to be isolated instead of existing in bundles. The SWNT diameter distribution spanned $\sim$0.9–1.5 nm, with Raman spectroscopy (488-nm excitation) indicating that the majority of the tubes have a 1.2-nm diameter. Further development of this HWCVD process to produce SWNTs at higher density is required. Coupling HWCVD production of carbon nanotubes with a simple purification process could result in an enabling technology for the development of nanotube composite or gas storage materials.

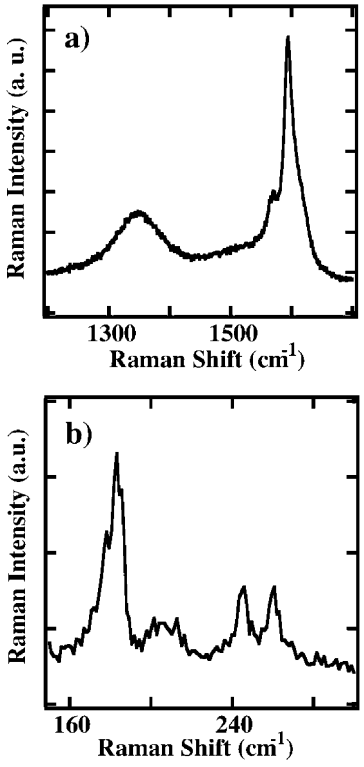

Fig. 3. Raman spectra of HWCVD SWNT material for (a) the nanotube tangential vibrational modes and (b) the radial breathing modes for laser excitation at 488 nm.

Acknowledgments

This work was supported by the DDRD program at NREL and by the Office of Science, Basic Energy Sciences, Division of Materials Science under subcontract DE-AC02-83CH10093.

References

[1] T. Ono, H. Miyashita, M. Esashi, Nanotechnology 13 (2002) 62.
[2] K.H. Park, K.M. Lee, S. Choi, S. Lee, K.H. Koh, J. Vac. Sci. Technol. B 19 (2001) 946.
[3] J.-h. Han, B.-S. Moon, W.S. Yang, J.-B. Yoo, C.Y. Park, Surf. Coat. Technol. 131 (2000) 93.
[4] Z.F. Ren, Z.P. Huang, J.W. Xu, J.H. Wang, P. Bush, M.P. Siegal, P.N. Provincio, Science 282 (1998) 1105.
[5] C.-F. Chen, C.-L. Lin, C.-M. Wang, Jpn. J. Appl. Phys. 41 (2002) L67.
[6] L. Marty, V. Bouchiat, A.M. Bonnot, M. Chaumont, T. Fournier, S. Decossas, S. Roche, Microelectron. Eng. 61/62 (2001) 485.
[7] A.H. Mahan, J.L. Alleman, M.J. Heben, P.A. Parilla, K.M. Jones, A.C. Dillon, Appl. Phys. Lett. 81 (2002) 4061.
[8] A.C. Dillon, A.H. Mahan, J.L. Alleman, P.A. Parilla, K.M. Jones, K.E.H. Gilbert, M.J. Heben, Appl. Phys. Lett. (submitted).
[9] B.P. Nelson, R.S. Crandall, E. Iwaniczko, A.H. Mahan, Q. Wang, Y. Xu, W. Gao, Mater. Res. Soc. Symp. Proc. 557 (1999) 97.
[10] A.C. Dillon, T. Gennett, K.M. Jones, J.L. Alleman, P.A. Parilla, M.J. Heben, Adv. Mater. 11 (1999) 1354.
[11] A.C. Dillon, P.A. Parilla, J.L. Alleman, J.D. Perkins, M.J. Heben, Chem. Phys. Lett. 316 (2000) 13.
[12] B.P. Nelson, Q. Wang, E. Iwaniczko, A.H. Mahan, R.S. Crandall, Mater. Res. Soc. Symp. Proc. 927 (1998) 507.
[13] A.M. Rao, E. Richter, S. Bandow, B. Chase, P.C. Eklund, K.A. Williams, S. Fang, K.R. Subbaswamy, M. Menon, A. Thess, R.E. Smalley, G. Dresselhaus, M.S. Dresselhaus, Science 275 (1997) 187.
[14] S. Bandow, S. Asaka, Y. Saito, A.M. Rao, L. Grigorian, E. Richter, P.C. Eklund, Phys. Rev. Lett. 80 (1998) 3779.